Quantum theory of coherent transverse optical magnetism

Stephen C. Rand

Division of Applied Physics, University of Michigan, Ann Arbor, Michigan 48109 (scr@umich.edu)

Received June 18, 2009; accepted September 14, 2009;
posted September 23, 2009 (Doc. ID 112946); published November 3, 2009

Density matrix theory is presented to explain recent experimental observations of intense optically induced magnetism due to a "mixed" type of nonlinearity proportional to the product of the electric- and magnetic-field strengths of light. Two previously unknown quadratic optical effects are predicted—namely, transverse optical magnetization and magnetic charge separation—and quantitative agreement is obtained with experimental results regarding the former of these. The mechanistic origin of a third quadratic nonlinearity, namely, magneto-electric second-harmonic generation, which is familiar on a phenomenological basis in classical nonlinear optics, is also examined. Transverse optical magnetism is shown to enable large permeability changes at optical frequencies accompanied by magnetic dispersion near resonances. This phenomenon provides for all-optical generation of magnetic moments, large transverse magnetic fields, static electric dipoles, and terahertz radiation in (unbiased) transparent homogeneous dielectrics or semiconductors. Intriguing possibilities for applications are considered, including magneto-electric refractive index modification, optical electric power generation, and spin control.

OCIS codes: 190.0190, 190.4410, 190.7110, 320.7120.

1. INTRODUCTION

Throughout the long history of nonlinear optics, an enormous number of phenomena have been discovered in which electromagnetic waves combine to alter the properties of materials in complex ways. Nonlinear interactions proportional to various powers of the incident electric fields (E^2, E^3, etc.) have contributed greatly to the emergence of entire scientific fields such as ultrafast photochemistry, quantum optics, holography, quantum information, spintronics, and laser cooling. Although nonlinear optics is now a mature topic, the possibility of having the magnetic field of light work in concert with the electric component to yield a nonlinear *magnetic* response proportional to the product of electric and magnetic field strengths has gone unnoticed. Longitudinal magneto-optic effects such as the Faraday and inverse Faraday effect are well documented, but transverse magneto-electric (EH) effects in which both contributing fields oscillate at the optical frequency are unknown. In the past, the strength of magnetic dipole interactions was invariably thought to be limited to a small fraction of that of electric dipole interactions. Following a recent discovery [1], however, new geometries have become available for all-optical interactions and magnetic device applications that provide unexpectedly direct ways of controlling spins and creating magnetic moments in ordinary matter. An entirely new class of nonlinear optical interactions is emerging that holds promise for unanticipated electromagnetic technologies based on natural materials. This article formulates the quantum theory of this class of effects against the backdrop of recent observations of transverse optical magnetism.

Recently published experiments [1–3] and classical analysis [2] have revealed a quadratic mechanism whereby intense magneto-electric response can be obtained in (nominally nonmagnetic) dielectric media. Magnetic dipole emission nearly as intense as the electric polarization has been reported at infrared and visible wavelengths in transparent dielectric liquids (CCl_4, C_6H_6, and H_2O), far from any electronic resonances. Although the possibilities for magneto-electric material modification with light are expected to be more dramatic on resonance, where a quantum mechanical analysis is required, no quantum treatment of this problem has appeared. Here an analysis is made of the parametric origin of intense magnetic dipole emission and magnetization induced by linearly polarized optical waves in bound electron systems using the density matrix. This theory is in quantitative accord with experiments performed to date at nonrelativistic intensities in several insulators. Furthermore, it predicts the possibility of magneto-electric modification of the index of refraction in low-loss natural materials, and introduces a novel approach to generate intense magnetic fields that may be of use in many disciplines that rely on spin physics.

Since the time of Maxwell [4], it has been widely accepted that the effects of the magnetic component H of light can be ignored compared to effects of the electric component E at ordinary intensities. Though magnetic phenomena exhibit close parallels to electric behavior at relativistic intensities, strong magnetic response is absent in the optical range under moderate irradiation conditions. This has been attributed in the past to the comparative weakness of the (optical) magnetic Lorentz force. Arguments have been made suggesting that, unlike the electric permittivity ε, the magnetic permeability μ loses even its physical meaning at optical frequencies [5]. Consequently, the many possibilities available through non-

linear optics for controlling the propagation of electromagnetic waves by altering the permittivity $\varepsilon(\omega,E,H)$ with external fields were thought not to extend to the permeability $\mu(\omega,E,H)$. In natural materials, where μ typically has the value μ_0 characteristic of vacuum, it appeared that *arbitrary* control over the spatial properties of waves that depend in principle on both ε and μ was impossible. Until now, controlled variation of magnetic permeability even at relatively low frequencies in the gigahertz range has been realizable only in artificial materials called metamaterials [6]. Experimental research on transformation optics [7,8], which calls for controlled spatial variations of ε and μ together with low losses at much higher frequencies, therefore faces even greater challenges. In this paper, however, a new mechanism is analyzed that is capable of generating intense magnetic fields at single points, or along surfaces or in macroscopic volumes, and allows precise control of magnetic dispersion in low-loss, homogeneous dielectrics. The magnetic fields and dipole moments resulting from transverse optical magnetism are derived in subsequent sections, and then their possible relevance is considered to next-generation magnetic memories [9], spintronics [10], control of spins in Bose–Einstein condensates [11], atom optics [12], quantum information science [13], and electric power generation.

Research performed in transparent dielectrics (water, CCl_4, and benzene) at optical intensities as low as $I \sim 10^8$ W/cm^2, fully ten orders of magnitude below the relativistic optics threshold of $I \sim 10^{18}$ W/cm^2, has now provided experimental evidence of a second-order magneto-electric optical process capable of generating intense magnetic dipole emission [1–3]. The measured magnetic susceptibility can be as large as half the electric dipole susceptibility, even far from any electronic resonances. Classical theory [2] that accounts for these surprising effects through the leading term of the multipole expansion, and predicts many new magneto-optical phenomena, agrees with these observations. However a quantum mechanical analysis of transverse optical magnetism has not yet been provided.

The main purpose of this paper is, therefore, to formulate a quantum mechanical theory of the intense transverse magnetic dipole moments and static electric dipole moments that form in bound electron systems as the result of irradiation with coherent light of moderate intensity. A radiant magnetization that is driven simultaneously by the optical electric and magnetic fields is first calculated analytically using density matrix analysis of 2-level atoms or molecules. The calculation shows that directly driven magnetic resonance is possible, and by considering the induced magnetic dispersion near an electronic resonance, predictions are made of intensity-dependent, magnetic modifications of the refractive index in dielectric media. We show that it is theoretically possible to attain negative permeability in natural materials that are completely homogeneous, and that moderately intense light can be used to program the spatial distribution of $\mu(I,\omega)$. We further deduce that static charge separation takes place under the same conditions, and we mention briefly the prospect of electric power generation in transparent insulators.

2. DENSITY MATRIX ANALYSIS

We begin by considering a system of identical 2-level atoms or molecules with a resonance frequency $\omega_0=(\omega_2-\omega_1)$ subjected to an electromagnetic plane wave of frequency ω that propagates in the positive z direction. The light is linearly polarized along $\hat{x}$ and detuned from resonance by $\Delta \equiv \omega_0-\omega$. Population dynamics and coherences are found using the density matrix equation of motion:

$$i\hbar\dot{\rho} = [H,\rho] - i\hbar\dot{\rho}_{relax}. \tag{1}$$

The system Hamiltonian $H=H_o+V(t)$ is assumed to consist of a static part,

$$H_o = \hbar\omega_1|1\rangle\langle 1| + \hbar\omega_2|2\rangle\langle 2|, \tag{2}$$

which describes the unperturbed diagonal matrix elements of the static Hamiltonian and an optical interaction V of the combined dipole form

$$V = -\bar{\mu}_e\cdot\bar{E} - \bar{\mu}_m\cdot\bar{B}. \tag{3}$$

In the semiclassical approach used here, $\dot{\rho}_{relax}$ describes phenomenological relaxation of individual density matrix elements in the Schrödinger picture. Uppercase rate constants Γ_{ij} are used to describe coherence decay between levels i and j and lowercase constants γ_{ii} give the total population decay rate of a particular level i. The irreducible representations of the (polar) electric and (axial) magnetic components of the optical wave are

$$\bar{E}(t) = -\frac{1}{2}[E_+\hat{\varepsilon}_- + E_-\hat{\varepsilon}_+]e^{i\varphi} + h.c., \tag{4}$$

$$\bar{B}(t) = -\frac{i}{2}[B_+\hat{\varepsilon}_- - B_-\hat{\varepsilon}_+]e^{i\varphi} + h.c.. \tag{5}$$

In these expressions $\varphi \equiv \omega t - kz$ is the optical phase and the circular basis vectors $\hat{\varepsilon}_\pm = -(\hat{x}\pm i\hat{y})/\sqrt{2}$ are components of the rank one spherical tensor. *h.c.* is an abbreviation for Hermitian conjugate. Carets are used throughout this paper to denote unit basis vectors. In the case of linear polarization along $\hat{x}$, we note the correspondences

$$E_+ = E_- = E_0/\sqrt{2} \tag{6}$$

and $B_+=B_-=B_0/\sqrt{2}$, which assume the circular components have equal amplitudes. The irreducible electric and magnetic dipole moments induced by the field have magnitudes and directions given by

$$\bar{\mu}^{(e)} = -(\mu_-^{(e)}\hat{\varepsilon}_+ + \mu_+^{(e)}\hat{\varepsilon}_-), \tag{7}$$

and

$$\bar{\mu}^{(m)} = -i(\mu_+^{(m)}\hat{\varepsilon}_- - \mu_-^{(m)}\hat{\varepsilon}_+), \tag{8}$$

respectively. When the circular components $\mu_\pm$ of these moments are equal, the electric and magnetic moments themselves point along $\hat{x}$ and $\hat{y}$—parallel to the inducing fields.

Substitution of Eqs. (4)–(8) into Eq. (3) furnishes the irreducible form of the interaction Hamiltonian. The use of Eqs. (2) and (3) in Eq. (1) then permits solution of the density matrix $\rho(t)$. The main purpose of this paper is to pre-

dict the temporal behavior of induced electric and magnetic dipole moments in the medium by calculating the expectation values $<\mu^{(e)}(t)>=Tr\{\mu^{(e)},\rho(t)\}$ and $<\mu^{(m)}(t)>=Tr\{\mu^{(m)},\rho(t)\}$, respectively.

3. MATRIX ELEMENTS OF TRANSVERSE MAGNETIC MOMENTS

Before proceeding to solve the equation of motion for the density matrix, a discussion of the calculation of expectation values is warranted due to the transverse nature of the magnetic dipole moment to be considered here. Individual light quanta carry spin angular momentum with projections on the axis of propagation given by $-\hbar$, $+\hbar$, or 0, depending on whether their state is left-circular, right-circular, or linear polarization respectively. In linear single-field MD interactions, the angular momentum needed to create or destroy a magnetic dipole moment is therefore provided by an appropriate state of circularly polarized incident light. However, in what follows, the induced angular momentum is not along $\hat{z}$, which denotes the propagation axis, but along the optical B field (chosen here to point along the transverse $\hat{y}$ direction). The induced transverse moment, therefore, has no projection on the axis of propagation and can be generated without the transfer of any angular momentum from the optical field. For the quadratic interaction of interest here, it will be shown that when the angular momentum of the light field is *zero* (the case of linearly polarized light), a large magnetic moment that oscillates at the optical frequency itself can be induced perpendicular to $\hat{z}$. The time average value of this orbital angular momentum is zero so that angular momentum is conserved overall. However, this process gives rise to intense, radiant magnetic dipole fields.

To facilitate a comparison of longitudinal and transverse magnetic moments, it is convenient to consider two coordinate systems in which the polar axis is either parallel or perpendicular to the wavevector $\bar{k}=k\hat{z}$. First we discuss longitudinal magnetic moments by considering the coordinate system (r,θ,φ) in which the polar and quantization axes are parallel to $\hat{k}=\hat{z}$, and the azimuthal angle φ is measured with respect to the x axis. This is the geometry of conventional magnetic dipole transitions. The electric dipole transition moment on a single atom is

$$\begin{aligned}\langle\bar{\mu}^{(e)}(t)\rangle_{12}&=\hat{r}\langle\mu^{(e)}(t)\rangle_{12}\\&=\hat{r}\int dV\psi_1^*(r,t)er\psi_2(r,t)+h.c.\\&=\hat{r}\int dVc_1^*(t)\psi_1^*(r)erc_2(t)\psi_2(r)+h.c.\\&=\hat{r}\langle 1|\mu^{(e)}|2\rangle\rho_{21}(t)+h.c.\end{aligned}\tag{9}$$

The electric field along $\hat{x}$ changes only the radial coordinate r of charge position. Thus $\hat{r}=\hat{x}$, and the expectation value of the electric dipole is

$$\langle\bar{\mu}^{(e)}\rangle=Tr\{\bar{\mu}^{(e)},\rho\}=\hat{x}(\mu_{12}\rho_{21}+\mu_{21}\rho_{12}),\tag{10}$$

where $\mu_{12}^{(e)}=\langle 1|\mu^{(e)}|2\rangle$ and $\rho_{21}(t)=c_1^*(t)c_2(t)$. The trace in Eq. (10) is, in general, a sum over all states of the system. Here however, we assume that the dynamics are dominated by only two states. State 1 is the ground state and state 2 denotes the particular excited state that has minimum detuning from the incident light frequency and opposite parity with respect to state 1. The quantities c_1 and c_2 are the probability amplitudes of state 1 and state 2, respectively.

The magnetic dipole transition moment for a one-photon interaction connecting states 1 and 2 is

$$\begin{aligned}\langle\bar{\mu}^{(m)}(t)\rangle_{12}&=(e/2m)\int dV\psi_1^*(r,\theta,\varphi,t)\bar{r}\times\bar{p}\,\psi_2(r,\theta,\varphi,t)+h.c.\\&=(e/2m)\int dVc_1^*(t)\psi_1^*(r,\theta,\varphi)\bar{L}c_2(t)\psi_2(r,\theta,\varphi)+h.c.\end{aligned}\tag{11}$$

in terms of the angular momentum operator $\bar{L}=\bar{r}\times\bar{p}$. In this case, the expectation value is given by the trace of the magnetic dipole operator $\bar{\mu}^{(m)}=(e/2m)\bar{L}$ with the density matrix:

$$\langle\bar{\mu}^{(m)}\rangle=\langle 1|\bar{\mu}^{(m)}|2\rangle\rho_{21}(t)+h.c.=Tr\{\bar{\mu}^{(m)},\rho\}.\tag{12}$$

At low intensities the magnetic moment in Eq. (12) is negligible for linear polarization, because the linear momentum $\bar{p}$ of the electron is very nearly parallel to its displacement. The Lorentz force is negligible compared to the force of the electric field at nonrelativistic intensities. The cross product in the integrand of Eq. (11) and the associated angular momentum are therefore nearly zero. Only an electric dipole oriented along $\hat{x}$ is induced. In the case of circular polarization, the electron follows the electric field adiabatically, circulating around the propagation axis, inducing a steady magnetic moment oriented along the z axis ($\bar{r}\times\bar{p}\neq 0$). This motion mediates the inverse Faraday effect caused by circularly polarized light [14], which is not of interest in this paper. Consequently, in one-photon, electric-field-mediated interactions, only the angular momentum carried by the field $E(z,t)$, where z is the quantization axis, can be transferred to the atom and the initial and final states $|1\rangle$ and $|2\rangle$ must differ in magnetic quantum number m accordingly ($m_2=m_1\pm 1$).

In the case of an interaction mediated jointly by the E and B components of a linearly polarized field, the orientation of the magnetic moment is along the laboratory y axis, and its calculation is significantly different because two driving forces contribute to the motion. The Lorentz force causes the linear momentum induced by the electric field E to acquire a small transverse component that is azimuthal with respect to the B component of the optical field. We therefore introduce new source coordinates (r',θ',φ') with a polar axis along B ($\hat{z}'=\hat{y}$). As before E defines the $\hat{x}'=\hat{x}$ axis. The third basis vector is $\hat{y}'=-\hat{z}$, and φ' is considered to be measured from the $\hat{y}'$ axis. In this primed coordinate system the linear momentum may be written as $\bar{p}'=\hat{r}'p_{r'}+\hat{\theta}'p_{\theta'}+\hat{\varphi}'p_{\varphi'}$. The expression for the magnetic moment in Eq. (11) becomes

$$\langle \bar{\mu}^{(m)}(t)\rangle_{12} = (e/2m)\int dV' \psi_1^*(r',\theta',\varphi',t)\bar{r}' \times[\bar{p}_{r'}+\bar{p}_{\theta'}+\bar{p}_{\varphi'}]\psi_2(r',\theta',\varphi',t) + h.c. = \frac{-e}{2m}\hat{y}\int dV' \psi_1^*(r',\theta',\varphi',t)\bar{r}' p_{\varphi'}\psi_2(r',\theta',\varphi',t) + h.c., \quad (13)$$

since $\hat{r}'\times\bar{p}_{r'}=0$ and $\hat{r}'\times(p_{\varphi'}\hat{\varphi}')=-p_{\varphi'}\hat{y}$. Here the assumptions have been made that $p_{\theta'}\cong 0$ (since neither field drives motion in the $\hat{\theta}'$ direction) and that r' is sufficiently slowly varying so that the amplitude of an oscillatory magnetic moment can be well defined and slowly varying too. Equation (13) is implicitly written in the rotating frame where the rapid time dependence is associated with the azimuthal momentum $p_{\varphi'}$ and the magnetic moment points in the expected direction anti-parallel to the B field (along $-\hat{y}$).

Under the action of the forces due to orthogonal fields E and B, the time dependence of radial ($\hat{r}'$) and azimuthal ($\hat{\varphi}'$) motions may differ. Hence we assume the wavefunction is separable according to $\psi(r',\theta',\varphi',t)=\psi(r',t)\psi(\theta',\varphi',t)$ and introduce separate c coefficients for the radial and angular parts of the wavefunction as follows: $\psi(r',t)=c^{(e)}(t)\psi(r')$ and $\psi(\theta',\varphi',t)=c^{(m)}(t)\psi(\theta',\varphi')$. Correspondingly, we define electric and magnetic density *sub-matrices* by $\rho_{ij}^{(e)}=c_j^{*(e)}c_i^{(e)}$ and $\rho_{ij}^{(m)}=c_j^{*(m)}c_i^{(m)}$ in the laboratory reference frame. The time development of $\rho_{ij}^{(e)}$ is determined by E, and that of $\rho_{ij}^{(m)}$ is determined by B. Both fields oscillate at the optical frequency, so by invoking the slowly varying envelope approximation (SVEA) the two submatrices can be written in the lab frame as

$$\rho^{(e)}(t)=\tilde{\rho}^{(e)}e^{i\omega t} \quad (14)$$

and

$$\rho^{(m)}(t)=\tilde{\rho}^{(m)}e^{\pm i\omega t}, \quad (15)$$

where $\tilde{\rho}^{(e)}$ and $\tilde{\rho}^{(m)}$ designate the slowly varying amplitudes of the electric and magnetic coherences.

In terms of these quantities, the expression for the transverse magnetic moment in Eq. (13) becomes

$$\langle \bar{\mu}^{(m)}(t)\rangle = -\hat{y}\langle 1|\mu^{(m)}|2\rangle\rho_{21}^{(m)}(t)\tilde{\rho}_{21}^{(e)} + h.c., \quad (16)$$

where we have made the replacement $\langle 1|\mu^{(m)}|2\rangle = \langle 1|(e/2m)r'p_{\varphi'}|2\rangle$. According to Eq. (16), when the direction of the magnetic field is fixed along $\hat{y}$, the expectation value for the transverse magnetic moment is given by

$$\langle \bar{\mu}^{(m)}(t)\rangle = -\hat{y}Tr\{\mu^{(m)},\rho^{(m)}(t)\tilde{\rho}^{(e)}\}. \quad (17)$$

The main time dependence in this expression for the magnetic moment is associated with $\rho_{21}^{(m)}(t)$ in the rotating frame. The envelope of the electric contribution designated by $\tilde{\rho}_{21}^{(e)}$ is assumed to vary little during an optical period. The submatrices $\rho^{(m)}(t)$ and $\rho^{(e)}(t)$ are designated as magnetic and electric, using the superscripts m and e, because the former describes temporal evolution that is azimuthal with respect to the axis of the optical H field, while the latter describes radial oscillations of the wavefunction in the direction of E.

Note that the expectation value of the magnetic moment in Eq. (16) is second order in the wavefunction as expected, not fourth order. The full density matrix is just the product of the submatrices $\rho^{(m)}(t)$ and $\rho^{(e)}(t)$, given explicitly by

$$\rho = |\psi\rangle\langle\psi| = |\psi(r,t)\rangle|\psi(\theta,\varphi,t)\rangle\langle\psi(\theta,\varphi,t)|\langle\psi(r,t)| = \rho^{(m)}(t)\rho^{(e)}(t). \quad (18)$$

The submatrices $\rho^{(e)}(t)$ and $\rho^{(m)}(t)$ merely describe important degrees of freedom in the overall motion driven by applied fields E and B. In the next section these kinematically distinct submatrices are separately evaluated in order to calculate the induced magnetization and other moments that result from combined electric and magnetic forces.

4. STEADY-STATE SOLUTION OF THE DENSITY MATRIX

To write the total magneto-optical interaction consistent with any particular choice of reference frame requires some care. The reason for this is that interactions driven by EB involve motional effects of two orthogonal fields, one of which is a polar vector ($E(t)$) and the other of which ($B(t)$) is axial. The rotating frame of linear optical interactions governed by $E(t)$ alone, for example, has an axis along $\hat{z}$, whereas the magnetic moment induced by the combined action of $E(t)$ and $B(t)$ involves currents circulating about the $\hat{y}$ axis. In this paper the joint effect of the electric and magnetic interactions will ultimately be described in the lab frame of reference, but to provide perspective on the kinematics, use will be made of a sequence of three reference frames. The calculation of dynamics begins in the rotating frame, is next transformed to the ordinary lab frame, and finally ends up in a z-adjusted lab frame.

Customarily, the rotating wave approximation is introduced in optical analysis to solve for system dynamics. One result of this is that in the frame co-rotating with a circular component of $E(t)$, the induced electric dipole is a constant. For this reason the electric dipole interaction is written as $-\bar{\mu}^{(e)}\cdot\bar{E}(t)$, where only the field varies with time. However, in the same reference frame, the magnetic moment oscillates at the optical frequency. This is implied by Eqs. (15) and (17) where magnetic charge oscillation varies rapidly with time as $\rho_{21}^{(m)}\propto\exp(\pm i\omega t)$ whereas the electric coherence is only slowly varying. To include electric and magnetic interactions in an atom-field Hamiltonian referenced to a single frame, this must be taken into account.

The interaction Hamiltonian in the rotating frame has the form

$$V(t) = -\frac{1}{2}\hbar[(\Omega_+^{*(m)}+\Omega_-^{*(m)}) + (\Omega_+^{(e)} + \Omega_+^{(m)}e^{i\varphi})e^{i\varphi} + (\Omega_-^{(e)}+\Omega_-^{(m)}e^{-i\varphi})e^{-i\varphi}] + h.c. \quad (19)$$

Here $\Omega_\pm^{(e)}\equiv\mu_\mp^{(e)}E_\pm/\hbar$ and $\Omega_\pm^{(m)}\equiv\mu_\mp^{(m)}B_\pm/\hbar$ are the electric

and magnetic interaction terms for positive or negative (±) helicity. The time dependence of the magnetic interaction either adds to or subtracts from that of the electric field, and produces interaction terms at frequencies of 0 and 2ω as shown by Eq. (19). The electric and magnetic transition matrix elements of V are therefore

$$V_{12}^{(e)} \equiv \langle 1|V^{(e)}|2\rangle = -\frac{1}{2}\hbar\langle 1|[\Omega_+^{(e)} + \Omega_-^{*(e)}]e^{i\varphi} + h.c.|2\rangle \quad (20)$$

and

$$V_{12}^{(m)} \equiv \langle 1|V^{(m)}|2\rangle = -\frac{1}{2}\hbar\langle 1|[\Omega_+^{*(m)} + \Omega_-^{*(m)}] + h.c.|2\rangle$$
$$-\frac{1}{2}\hbar\langle 1|[\Omega_+^{(m)} + \Omega_-^{*(m)}]e^{2i\varphi} + h.c.|2\rangle. \quad (21)$$

The charge oscillations induced by an electric field acting alone follow the time dependence of E. Hence the electric-field-induced coherence has the form $\rho_{12}^{(e)}(t) = \tilde{\rho}_{12}^{(e)}e^{i\varphi}$ in the lab frame or $\rho_{12}^{(e)}(t) = \tilde{\rho}_{12}^{(e)}$ in the rotating frame, as previously indicated in Eq. (14). Charge oscillations that are jointly driven by electric and magnetic forces similarly follow the time dependence of the applied fields, and this gives rise to three distinct frequencies of oscillation in the lab frame, namely, 0 and $\pm 2\omega$, because there are combination terms in the product of the driving fields E and B.

$$E(t)B(t) = \left\{\frac{1}{2}[E_0\hat{x}]e^{i\varphi} + h.c.\right\}\left\{\frac{1}{2}[B_0\hat{y}]e^{i\varphi} + h.c.\right\}$$
$$= \frac{1}{4}\{E_0B_0e^{2i\varphi} + E_0^*B_0^*e^{-2i\varphi} + E_0B_0^* + E_0^*B_0\}. \quad (22)$$

The coherence in Eq. (18) is therefore expected to take the form

$$\rho_{12}(t) = \tilde{\rho}_{12}^{(m)*}(\omega)\tilde{\rho}_{12}^{(e)}(\omega) + \tilde{\rho}_{12}^{(m)}(\omega)\tilde{\rho}_{12}^{(e)}(\omega)e^{2i\varphi} = \tilde{\rho}_{12}(\omega = 0)$$
$$+ \tilde{\rho}_{12}(2\omega)e^{2i\varphi} \quad (23)$$

in the lab frame. Notice that the terms on the right of Eq. (23) have the same time dependence as those in the magnetic interaction Hamiltonian of Eq. (21) and agree with the lab frame product of the magnetic and electric submatrices given by Eqs. (14) and (15).

Equation (1) may now be solved directly for steady-state solutions by setting $\dot{\tilde{\rho}}_{12}^{(e)} = \dot{\tilde{\rho}}_{12}^{(m)} = 0$. We treat the electric interaction exactly, by applying it as a strong field in zeroth order ($V^{(0)}(t) = -\bar{\mu}^{(e)}\cdot\bar{E}(t)$). The magnetic dipole interaction is then applied as a perturbation in concert with the electric dipole interaction in first order ($V^{(1)} = -\bar{\mu}^{(e)}\cdot\bar{E}(t) - \bar{\mu}^{(m)}(t)\cdot\bar{B}(t)$), and the equation of motion is solved for the submatrix coherences by collecting terms at each frequency.

This procedure yields first-order results for the coherences, which are

$$\rho_{12}^{(e)} = \frac{1}{2}\left\{\frac{[\Omega_+^{(e)} + \Omega_-^{*(e)}]_{12}}{(\Delta_1 + i\Gamma_{12})}e^{i\omega t}\right\}(\rho_{11} - \rho_{22}), \quad (24)$$

$$\rho_{12}^{(m)} = \frac{1}{2}\left\{\frac{[\Omega_+^{\prime(m)} + \Omega_-^{\prime(m)}]_{12}}{(\omega_0 + i\Gamma_{12}^{(m)})}e^{-i\omega t}\right.$$
$$\left. + \frac{[\Omega_+^{(m)} + \Omega_-^{*(m)}]_{12}}{(\Delta_2 + i\Gamma_{12}^{(m)})}e^{i\omega t}\right\}(\rho_{11}^{(0)} - \rho_{22}^{(0)}), \quad (25)$$

in the lab frame. Here the counter-rotating magnetic amplitude that gives rise to the time-independent term in Eq. (25) is designated by $\Omega_\pm^{\prime(m)} \equiv \mu_\mp^{(m)}B_\pm^*/\hbar$. The detunings in the resonant denominators are defined by $\Delta_1 \equiv \omega_0 - \omega$ and $\Delta_2 \equiv \omega_0 - 2\omega$. In obtaining Eq. (25) the magnetic interaction has been treated as a perturbation, so the population difference equals the initial value, which may be assumed to correspond to the ground state ($\rho_{11}^{(0)} - \rho_{22}^{(0)} = 1$). Population saturation effects due to the electric interaction are nevertheless taken into account when the electric field interaction is applied a second time to obtain the first-order result. The population difference $(\rho_{11} - \rho_{22})$ that appears in Eq. (24) is then given by

$$\rho_{11} - \rho_{22} = \left[1 + \frac{\Gamma_{12}^{(e)}|\Omega_+^{(e)} + \Omega_-^{*(e)}|^2}{\gamma_{22}(\Delta_1^2 + \Gamma_{12}^{(e)2})}\right]^{-1}. \quad (26)$$

5. CALCULATION OF TRANSVERSE OPTICAL MAGNETIZATION

The steady-state solution for the magnetization $\bar{M}$—the same macroscopic magnetization that appears in the constitutive relation $\bar{B} = \mu_0(\bar{H} + \bar{M})$ associated with Maxwell's equations—is given in the lab frame by

$$\bar{M} = NTr\{\bar{\mu}^{(m)}(t), \rho(t)\}$$
$$= NTr\{\bar{\mu}^{(m)}(t), \rho^{(m)}(t)\rho^{(e)}(t)\}$$
$$= -N\hat{y}[\langle 2|\mu^{(m)}(t)|1\rangle\rho_{12}^{(m)}(t)\rho_{12}^{(e)}(t) + h.c]. \quad (27)$$

Here $\bar{M}$ is referenced to laboratory coordinates (x,y,z), which parallel the directions of E, B, and the propagation axis, respectively. Shortly we shall transform to a z-corrected lab frame with coordinates (x,y,z) in which the theory can be compared directly with experiments that involve projections of circular currents on the x and z axes.

With the results of Eqs. (24) and (25) in hand, we now specialize to the case of linear polarization. Upon substitution of the coherences (24) and (25) into Eq. (27), the magnetization of Eq. (27) yields the result

$$\bar{M}(t) = -\hat{y}\left(\frac{Ne}{2m}\right)\left\{\frac{1}{2}\left[\frac{\langle 2|L_y|1\rangle[\Omega_0^{(e)}]_{12}[\Omega_0^{(m)}]_{12}}{(\Delta_1 + i\Gamma_{12}^{(e)})(\Delta_2 + i\Gamma_{12}^{(m)})}e^{i\omega t}\right.\right.$$
$$\left.\left. + \frac{\langle 2|L_y|1\rangle[\Omega_0^{(e)}]_{12}[\Omega_0^{\prime(m)}]_{12}}{(\omega_0 + i\Gamma_{12}^{(e)})(\Delta_2 + i\Gamma_{12}^{(m)})}e^{-i\omega t}\right] + h.c.\right\}(\rho_{11} - \rho_{22}). \quad (28)$$

This expression is valid in the lab frame where $\mu_{21}^{(m)} \propto e^{-i\omega t}$. The field factors are $\Omega_0'^{(m)} = \mu_0^{(m)} B_0^*/\hbar$, $\Omega_0^{(m)} = \mu_0^{(m)} B_0/\hbar$, and $\Omega_0^{(e)} = \mu_0^{(e)} E_0/\hbar$. Only one circular component of the electric field interaction contributes to $\bar{M}(t)$, whereas both circular components of the magnetic interaction participate. Hence the specific replacement $\Omega_0^{(m)} = [\Omega_+^{(m)} + \Omega_-^{*(m)}]$ has been made for the magnetic term, and $\Omega_0^{(e)} = \frac{1}{2}[\Omega_+^{(e)} + \Omega_-^{*(e)}]$ for the electric term. This consideration removes one factor of 2 from the denominator of the expression for $\bar{M}$.

The magnetization in Eq. (28) has the general form

$$\bar{M} = \frac{1}{2}\tilde{M}e^{i\varphi} + h.c., \tag{29}$$

where the slowly varying amplitude $\tilde{M}$ is given by

$$\tilde{M} = -\hat{y}\left(\frac{Ne}{m}\right)\frac{1}{2}\left[\frac{\langle 2|L_y|1\rangle[\Omega_0^{(e)}]_{12}[\Omega_0^{(m)}]_{12}}{(\Delta_1 + i\Gamma_{12}^{(e)})(\Delta_2 + i\Gamma_{12}^{(m)})} + \frac{\langle 2|L_y|1\rangle^*[\Omega_0^{*(e)}]_{12}[\Omega_0'^{(m)*}]_{12}}{(\omega_0 - i\Gamma_{12}^{(e)})(\Delta_2 - i\Gamma_{12}^{(m)})}\right](\rho_{11} - \rho_{22}). \tag{30}$$

Notice that although the process giving rise to this magnetization is second order in the incident fields, the magnetic dipole in Eq. (29) oscillates at the fundamental frequency ω not 2ω.

Before we can determine the dimensionless ratio R of magnetic to electric-dipole moments as a function of incident field strength, we must account for the axial versus polar nature of MD and ED moments. An adjustment is needed to account for the fact that of all the electrons that can be set in motion by the electric field to produce polarization P within a given volume, at most one half can be deflected to contribute to a magnetic moment M in the same volume [2]. For a given number of charges per unit volume, the amplitude of the oscillatory magnetization must therefore be corrected by another factor of 2 before direct comparison with the amplitude of electric polarization is possible.

This correction is equivalent to a transformation $(x,y,z) \rightarrow (x,y,2z)$ that rescales the laboratory z coordinate, since oscillatory motion in an arc about B resolves itself differently on the Cartesian x and z axes (See [2] for further discussion). Circular arc motion projected onto $\hat{z}$ reverses twice as often as the same motion projected on $\hat{x}$. As a result, the amplitude of magnetic charge oscillations projected onto the propagation axis must be halved for comparison with the amplitude of electric dipole oscillation measured along $\hat{x}$. The halving of the z amplitude may be taken into account with the substitution $L_y \rightarrow 2L_y$ in Eq. (30). We also note that the second term in Eq. (30) is much smaller than the first due to the ω_0 factor in the denominator. To an excellent approximation our expression for the radiant magnetization at the optical frequency therefore reduces to

$$\tilde{M} = -\hat{y}N\left(\frac{e}{m}\right)\frac{\langle 2|L_y|1\rangle\Omega_0^{(e)}\Omega_0^{(m)}}{(\Delta_1 + i\Gamma_{12}^{(e)})(\Delta_2 + i\Gamma_{12}^{(m)})}(\rho_{11} - \rho_{22}). \tag{31}$$

The dimensionless ratio of magnetic to electric moments is therefore given by

$$R = \left|\frac{\tilde{M}}{c\tilde{P}}\right| = \left|\left(\frac{e}{mc}\right)\frac{\langle 2|L_y|1\rangle\tilde{\rho}_{12}^{(e)}\tilde{\rho}_{12}^{(m)}}{\langle 2|ex|1\rangle\tilde{\rho}_{12}^{(e)}}\right| = \left|\left(\frac{\langle 2|x(p_\varphi/mc)|1\rangle}{\langle 2|x|1\rangle}\right)\tilde{\rho}_{12}^{(m)}\right|. \tag{32}$$

Since the momentum $\langle p_\varphi\rangle$ of charge motion cannot exceed $\langle p_\varphi\rangle = mc$, the ratio of matrix elements in parentheses on the right side of Eq. (32) cannot exceed unity. Also, the maximum value of the off-diagonal matrix element $\tilde{\rho}_{12}^{(m)}$ is 1/2 (see Appendix A). So the ratio R has a maximum value that is

$$R_{\max} = 1/2. \tag{33}$$

Though not obvious from the form of Eq. (32), it is important to note that the ratio of magnetic to electric susceptibility can attain the maximum value $R_{\max} = 1/2$ given by Eq. (33) at *nonrelativistic* intensities. This may be demonstrated by direct numerical integration of the equations of motion [15] and is the subject of a forthcoming publication [16]. Ultrafast growth (on a timescale $\Delta t < 100$ fs [1,3]) of magnetic response takes place via energy transfer from electric field-induced linear motion along x, to the azimuthal motion initiated by the magnetic field along $\hat{\varphi}'$, and is due to the phenomenon of parametric resonance [17].

On the basis of Eqs. (29)–(33), the development to this stage can be summarized in a few points. The radiant magnetic emission *intensity* is predicted to be quadratic with respect to the input intensity. It may be enhanced by electronic resonance at $\Delta_1 = 0$ and is governed secondarily by a parametric detuning factor $[\Delta_2 + i\Gamma]^{-1}$. It can grow to a value of, at most, one fourth ($R_{\max}^2 = 1/4$) that of the electric dipole emission intensity. These findings are in excellent agreement with experimental results [1–3] at intensities ten orders of magnitude below the relativistic threshold.

To calculate the magnetic susceptibility, and to compare it with the electric susceptibility, we now make use of Eq. (31).

$$\chi^{(m)} = \frac{\tilde{M}}{H_0} = \left(\frac{-Ne}{mH_0}\right)\left[\frac{\langle 2|L_y|1\rangle\hbar\Omega_0^{(e)}\hbar\Omega_0^{(m)}}{\hbar^2(\Delta_1 + i\Gamma_{12}^{(e)})(\Delta_2 + i\Gamma_{12}^{(m)})}\right](\rho_{11} - \rho_{22}) = \left(\frac{-N\mu_0 e^3}{2m^2\hbar^2}\right)\left[\frac{|\langle 2|L_y|1\rangle|^2\langle 1|x|2\rangle}{(\Delta_1 + i\Gamma_{12}^{(e)})(\Delta_2 + i\Gamma_{12}^{(m)})}\right](\rho_{11} - \rho_{22})E_0. \tag{34}$$

The electric susceptibility $\chi^{(e)}$ may similarly be determined by comparing its defining relationship, namely,

$$P(t) = \frac{1}{2}\tilde{P}e^{i\omega t} + h.c. = \frac{1}{2}\varepsilon_0\chi^{(e)}(-\omega)E_0e^{i\omega t} + h.c., \tag{35}$$

with Eqs. (10) and (24). This yields

$$\tilde{P} = 2N\mu_{21}\tilde{\rho}_{12}^{(e)} = \left(\frac{Ne^2}{\hbar}\right)\left[\frac{|\langle 1|x|2\rangle|^2 E_0}{(\Delta_1 + i\Gamma_{12}^{(e)})}\right](\rho_{11} - \rho_{22}) \quad (36)$$

and

$$\chi^{(e)} = \left(\frac{Ne^2}{\varepsilon_0\hbar}\right)\frac{|\langle 2|x|1\rangle|^2}{(\Delta_1 + i\Gamma_{12}^{(e)})}. \quad (37)$$

In both the expressions (34) and (37), local field renormalization has been ignored. The ratio of magnetic and electric susceptibilities obtained from these results is

$$\frac{\chi^{(m)}(\omega)}{\chi^{(e)}(\omega)} = \left(\frac{-\mu_0\varepsilon_0 e}{2m^2\hbar}\right)\frac{|\langle 2|L_y|1\rangle|^2 E_0}{\langle 2|x|1\rangle(\Delta_2 + i\Gamma_{12}^{(m)})}$$
$$= \frac{-2}{\hbar c^2}\frac{|\langle 2|\mu^{(m)}|1\rangle|^2 E_0 e^{-i\varphi_p}}{\langle 2|\mu^{(e)}|1\rangle\sqrt{\Delta_2^2 + \Gamma_{12}^{2(m)}}}, \quad (38)$$

where $\varphi_p \equiv \tan^{-1}(\Gamma_{12}^{(m)}/\Delta_2)$. Note that, in the vicinity of electronic resonance where magnetic dispersion is largest, the magnetic linewidth is expected to be much less than the parametric detuning factor ($\Gamma_{12}^{(m)} \ll \Delta_2$). Therefore $\varphi_p \cong 0$ and the signs of electric and magnetic dispersion are opposite, as depicted in Fig. 1. The matrix element in the numerator of Eq. (38) reflects transformation of the magnetic susceptibility as a rotation $R(y)$ about the y axis. According to Eq. (34), the magnetic susceptibility is also proportional to the electric dipole transition moment. Hence the matrix elements $\langle 2|L_y|1\rangle$ and $\langle 1|x|2\rangle$ must both be nonzero for optical magnetization to be allowed, and the electric field amplitude E_0 must be large for it to be intense.

Some further comments about selection rules are in order. Explicit evaluation of the magnetic matrix element between states of well-defined total initial and final angular momentum l_1 and l_2, respectively, using the Wigner-Eckart theorem [18], yields

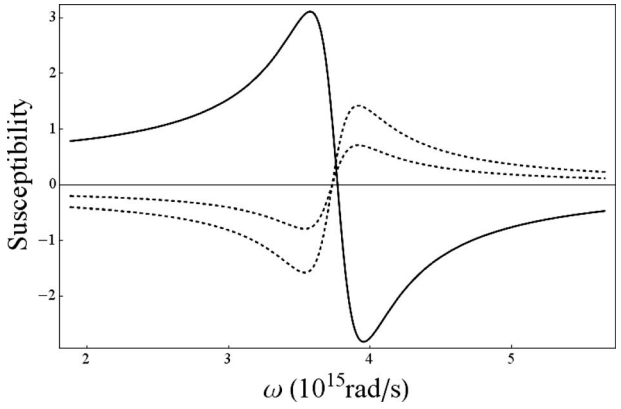

Fig. 1. Plot of the electric (solid curve) and magnetic (dashed curve) susceptibilities of a 2-level system with various proportions of optically induced magnetic dipole response. The horizontal axis corresponds to $\chi^{(m)}(\omega)=0$, and the dashed curves correspond to $\chi^{(m)}=-\chi^{(e)}(\omega)/4$ (upper curve at left), and $\chi^{(m)}=-\chi^{(e)}\times(\omega)/2$ (lower left). The linewidth-to-resonant-frequency ratio is $\Gamma/\omega_0=0.1$. All curves assume resonance at $\lambda_0=500$ nm and a plasma frequency of $\omega_p=2\times10^{15}$ rad·s^{-1}.

$$\langle 2|V_{\pm}^{(m)}|1\rangle = (-)^{l_2-m_2}\frac{1}{2}\{B_{\pm}\langle\alpha_2 l_2 m_2\|\mu_{\mp}^{(m)}\|\alpha_1 l_1 m_1\rangle + c.c.\}$$
$$\times\begin{pmatrix} l_2 & 1 & l_1 \\ -m_2 & q & m_1\end{pmatrix}. \quad (39)$$

Here α_1 and α_2 refer collectively to any quantum numbers other than l and m needed to specify the initial and final states exactly. MD and ED interaction matrix elements are proportional to the same 3-j symbol, but their reduced matrix elements transform as rotations about $\hat{y}$ and translations along $\hat{x}$, respectively. Equation (39) indicates explicitly that magnetic interactions induced by circularly polarized components of the B field ($q=\pm1$) exchange spin angular momentum of $\pm\hbar$ with the atom. By contrast, linearly polarized fields ($q=0$) exchange no spin angular momentum with the atom. Nevertheless, at moderate intensities, the combined action of linearly polarized E and B fields can drive the formation of a parametrically enhanced, oscillating *transverse* orbital angular momentum as specified by Eq. (31). For this to happen, the reduced matrix elements of $R(y)$ and x must be simultaneously nonzero, and the selection rules $\Delta l=\pm1$ and $\Delta m=m_2-m_1=0$ must be satisfied.

6. SECOND-HARMONIC AND DC ELECTRIC DIPOLE PROCESSES

Electric dipole moments can also be generated by the joint action of optical E and B fields. Two additional processes emerge from this analysis by considering expectation values of the electric dipole operator in combination with the magneto-electric coherences developed in Eqs. (24) and (25). One process yields a radiant polarization at the second-harmonic frequency, and the other produces a static electric dipole in the direction of propagation of light.

We now consider electric dipole moments that develop perpendicular to $\hat{x}$ and $\hat{y}$. A z-directed, magnetically induced electric dipole moment is clearly distinct from either the linear electric dipole induced along $\hat{x}$ or the nonlinear magnetic dipole induced along $\hat{y}$. Its macroscopic polarization is calculated using

$$\bar{P} = NTr\{\bar{\mu}^{(e)}, \rho(t)\}, \quad (40)$$

where

$$\bar{\mu}^{(e)} = \mu_0^{(e)}\hat{z}. \quad (41)$$

By substituting Eqs. (24), (25), and (41) into Eq. (40), and specializing again to the case of linear input polarization, one finds in the Cartesian lab frame where the charge oscillation along z is at a doubled frequency (i.e., $[\mu_{21}^{(e)}]_z \propto e^{-2i\omega t}$) that

$$\bar{P}(t) = N\hat{z}(\mu_{21}^{(e)}\rho_{12}^{(m)}(t)\rho_{12}^{(e)} + h.c.)$$
$$= N\hat{z}\left\{\left(\frac{1}{2}\frac{\mu_{21}^{(e)}[\Omega_0'^{(m)}]_{12}[\Omega_0^{(e)}]_{12}}{(\Delta_1 + i\Gamma_{12}^{(e)})(\omega_0 + i\Gamma_{12}^{(m)})}e^{-2i\omega t} + h.c.\right)\right.$$
$$\left. + \left(\frac{1}{2}\frac{\mu_{21}^{(e)}[\Omega_0^{(m)}]_{12}[\Omega_0^{(e)}]_{12}}{(\Delta_1 + i\Gamma_{12}^{(e)})(\Delta_2 + i\Gamma_{12}^{(m)})} + h.c.\right)\right\}\ldots \quad (42)$$

This expression for the electric polarization driven jointly by E and B contains two terms of different frequency. The first is a field at 2ω that generates second-harmonic radiation. Unlike the magnetization at frequency ω in Eq. (31), the second-harmonic signal is longitudinally polarized and lacks the parametric resonance factor $[\Delta_2 + i\Gamma]^{-1}$, so it is expected to produce only weak emission perpendicular to the pump wave. The second term is a zero-frequency term that predicts a static charge separation induced by light in dielectric media illuminated by moderately intense coherent light. Since it originates from the oscillatory coherence in Eq. (23) and contains the same parametric denominator as the magnetization in Eq. (31), its magnitude is expected to be strongly enhanced. In ultrashort pulse interactions, this effect will therefore generate intense longitudinally polarized terahertz radiation, although conventional phase-matching of the output will not be possible.

These same optical effects were predicted previously using steady-state analysis of a classical model of electron motion subject to external electric and magnetic forcing fields and Hooke's law restoring forces [2]. The present density matrix treatment has the merit of identifying the relative intensities, detuning dependences, emission frequencies, selection rules, directionality and multipole character of these effects in an independent, systematic way that requires no interpretation and is valid near resonances.

7. MAGNETIC DISPERSION

As one example of an application of these findings, we now briefly discuss the dispersion of the magnetic dipole response calculated in Eqs. (28) and (38) and its connection with refractive index behavior. The refractive index of a medium is determined by the relative permittivity ε_r and permeability μ_r according to $n=\sqrt{\varepsilon_r\mu_r}$. Ordinarily the permeability of dielectrics is very close to the vacuum value $\mu_r=1$ at all frequencies, and because it is constant it does not contribute to dispersion of the index. However, through the intensity dependence of the magnetic susceptibility $\chi^{(m)}(I)$, the refractive index $n(I)=\sqrt{(1+\chi^{(e)})(1+\chi^{(m)}(I))}$ itself becomes intensity-dependent. $n(I)$ can therefore be modified using induced magnetic dispersion, particularly near electronic resonances [19].

$\chi^{(m)}(I)$ and $\chi^{(e)}$ have opposite signs and a small phase shift as illustrated in Fig. 1. Consequently, the main effect of magnetic dispersion is to reduce the refractive index. In addition, for a sufficiently sharp electronic resonance at $\omega=\omega_0$, there is a frequency range on the red (long wavelength) side of resonance where the optically induced permeability μ_r may acquire negative values.

In the figure, the dashed curves illustrate induced magnetic susceptibilities of different magnitudes, near a resonance at $\lambda_0=500$ nm. The linewidth-to-frequency ratio is arbitrarily taken to be $\Gamma/\omega_0=0.1$. The plasma frequency $\omega_p\equiv(Ne^2/\varepsilon_0 m_e)^{1/2}$ is assumed to be $\omega_p=2\times10^{15}$ rad/s, close to the value for silica. The ratio $R=|\chi^{(m)}(I)/\chi^{(e)}|$ of magnetic-to-electric susceptibility has a value determined by the incident intensity and lies between zero and $R_{\max}=1/2$. R is negligible at low intensities, grows linearly at intermediate intensities, and eventually reaches $R_{\max}$ at a "saturation" intensity I_{sat} that is material-dependent [3]. Above I_{sat} the magnetization ceases to grow quadratically, becoming merely proportional to the incident intensity rather than to its square. In this "saturation" regime, the magnetic susceptibility therefore maintains a *fixed proportionality* with respect to the electric susceptibility.

8. CONCLUSION

The main results of this paper are contained in Eqs. (31), (33), and (42). The first of these predicts that light of frequency ω induces a coherent oscillatory magnetization that radiates at frequency ω in bound electron systems. This dynamic magnetization M arises via a quadratic nonlinearity [20] driven by the product EB of the optical field amplitudes and can be comparable in magnitude to the electric polarization P at high but subrelativistic intensities. Equation (33) shows that the maximum ratio of magnetic-to-electric susceptibility is $R_{\max}=|\chi^{(m)}/\chi^{(e)}|=1/2$, without resorting to classical arguments based on geometric considerations or Maxwell's equations. Thus the maximum intensity of magnetic dipole emission from insulators, which depends on the square of the susceptibility, is predicted to be one fourth that from electric dipole polarization, which is in excellent quantitative agreement with experiments to date. The coherence established by this type of interaction also gives rise to two other nonlinear optical effects. The first term in Eq. (42) describes magnetically induced second-harmonic generation, in which the emitted electric field lies along $\hat{z}$, parallel to the propagation of the pump light. The second term is static charge separation. The orientation of the static electric dipole is again along $\hat{z}$. Finally, we note that, according to Eqs. (31) and (36), the calculated electric and magnetic susceptibilities have opposite signs across electronic resonances, indicating that the induced magnetic response is diamagnetic. As a result, the magnetic dispersion that accompanies transverse optical magnetization near resonances provides a unique new method of modifying the refractive index of unstructured dielectrics.

The enhancement of magnetic response by a factor close to the speed of light as described in this work is due to parametric resonance. This phenomenon manifests itself in Eqs. (31) and (42) through the doubled-frequency detuning parameter Δ_2, but its impact only becomes apparent in numerical simulations [16]. The result of this dynamic enhancement is that magnetic dipole response can be nearly as intense as the electric response at intensities far below the relativistic threshold [21] due to transfer of energy between the motions associated with the E and B components of the light field. Physically, this process requires both an electric dipole transition and a magnetic dipole transition to be driven on the atom simultaneously by linearly polarized incident light. It is therefore not surprising that the transverse MD and ED selection rules require that rotations about y transform the same way as translations along x, and the MD and ED transition moments must be nonzero for the same initial

and final states. This requirement is met for states of different parity in many crystallographic point groups.

In systems that satisfy these symmetry requirements, an important role can be anticipated for the manipulation of orbital and spin magnetism by optical waves. In a manner quite different from earlier experiments that demonstrated ultrafast control over magnetic moments without applying static magnetic fields [14,22–24], the present results explain how transverse coherent magnetization can generate magnetic moments that are eight to ten orders of magnitude larger than expected, and internal magnetic fields that are in the Tesla range, by a new process at subrelativistic intensities. Since optical modulators can provide real-time control of the intensity and frequency of light within large volumes of dielectric material, this finding may enable programmable transformation optics, prolongation of coherence times for spintronic circuitry, ultrafast reading and writing of magnetic memories, and a new family of magnetic sensors or imagers. The capability of creating large magnetic moments or torques at an optical focus in dense systems of bound electrons, including condensates, should provide new modalities of spin control for research. Short-period magnetic field distributions produced by intense standing waves of light may be useful for atom optics or free electron lasers operating at short wavelengths. The availability of programmable distributions of intense magnetic fields could be used to improve the fidelity of compact quantum information systems based on spin qubits. Furthermore, these results have significant implications for high-field and plasma science, as well as laser fusion, since they make it clear that in ultrafast pulse interactions magnetic dynamics cannot be ignored at pre-pulse intensities even ten orders of magnitude below the relativistic threshold on very short timescales. Finally, the existence of a mechanism whereby light causes static charge separation in nonconducting media has been outlined. This opens the door to both capacitive and inductive electric power generation using coherent light.

APPENDIX A

Here it is shown that the maximum value of an off-diagonal density matrix element in a 2-level system is one-half. Consider a system described by the wavefunction

$$|\psi\rangle = \sum_i c_i|i\rangle = \cos\theta|1\rangle + \sin\theta|2\rangle. \tag{A.1}$$

Assume that the system is closed so that $\Sigma|c_i|^2=1$. Now introduce the density matrix elements $\rho_{ij}\equiv c_i c_j^*$ and rewrite the closure expression as

$$Tr\{\rho\} = \sum_i \rho_{ii} = Tr\{\rho\} = 1. \tag{A.2}$$

The Cauchy–Schwarz inequality dictates that

$$\left|\sum_i c_i c_i\right|^2 \le \sum_j |c_j|^2 \cdot \sum_k |c_k|^2, \tag{A.3}$$

which in terms of density matrix elements becomes

$$\sum_{i,j} \rho_{ij}\rho_{ji} \le \sum_j \rho_{jj} \cdot \sum_k \rho_{kk} = Tr\{\rho\} \cdot Tr\{\rho\} = 1. \tag{A.4}$$

Writing this out explicitly, we find

$$(\rho_{11}^2 + \rho_{22}^2) + 2|\rho_{12}|^2 \le 1, \tag{A.5}$$

$$2|\rho_{12}|^2 \le 1 - (\rho_{11}^2 + \rho_{22}^2). \tag{A.6}$$

Now since $\rho_{11}^2=\cos^4\theta$ and $\rho_{22}^2=\sin^4\theta$, the minimum value of $(\rho_{11}^2+\rho_{22}^2)$, which yields the maximum value of $|\rho_{12}|$ in the inequality, may be found by setting its derivative with respect to θ is equal to zero:

$$\frac{\partial}{\partial\theta}(\rho_{11}^2(\theta) + \rho_{22}^2(\theta)) = -4\cos^3\theta\sin\theta + 4\sin^3\theta\cos\theta = 0. \tag{A.7}$$

This condition is $\sin\theta=\pm\cos\theta$, and the corresponding solutions for θ are given by

$$\theta = \pm\frac{(2n+1)\pi}{4}, \quad n = 0,1,2\ldots. \tag{A.8}$$

For these values of θ one finds the minimum sum of the squared populations to be

$$(\rho_{11}^2 + \rho_{22}^2)_{\min} = \frac{1}{2}. \tag{A.9}$$

Substitution of Eq. (A.9) into Eq. (A.6) yields $|\rho_{12}|_{\max}^2 \le 1/4$, or

$$|\rho_{12}|_{\max} \le \frac{1}{2}. \tag{A.10}$$

ACKNOWLEDGMENTS

The author gratefully acknowledges funding by the National Science Foundation (DMR-0502715 and CISE-0531086) and assistance in preparation of this paper by William Fisher and Yuwei Li. The author thanks the following individuals and institutions for hospitality during the course of this research: C. deAraujo at Universidade Federale de Pernambuco, O. Svelto at Politecnico di Milano, W. Sibbett at the University of St. Andrews, and C. Mirasso at the Universitat de les illes Balears.

REFERENCES AND NOTES

1. S. L. Oliveira and S. C. Rand, "Intense nonlinear magnetic dipole radiation at optical frequencies: molecular scattering in a dielectric liquid," Phys. Rev. Lett. **98**, 093901 (2007).
2. S. C. Rand, W. M. Fisher, and S. L. Oliveira, "Optically-induced magnetization in homogeneous, undoped dielectric media," J. Opt. Soc. Am. B **25**, 1106–1117 (2008).
3. W. M. Fisher and S. C. Rand, "Dependence of optically-induced magnetism on molecular electronic structure," J. Lumin. (2009), doi:10.1016/j.jlumin.2009.02.036.
4. J. C. Maxwell, "A dynamical theory of electromagnetic fields," *The Scientific Papers of James Clerk Maxwell* (Cambridge Univ. Press, 1890), pp. 526–597.
5. L. Landau, E. M. Lifshitz, and L. P. Pitaevskii, *Electrodynamics of Continuous Media*, 2nd ed. (Pergamon Press, 1984), pp. 268–270.
6. J. B. Pendry, A. J. Holden, D. J. Robbins, and W. J.

Stewart, "Magnetism from conductors and enhanced nonlinear phenomena," IEEE Trans. Microwave Theory Tech. **47**, 2075–2084 (1999).
7. U. Leonhardt, "Optical conformal mapping," Science **312**, 1777–1780 (2006).
8. J. B. Pendry, D. Schurig, and D. R. Smith, "Controlling electromagnetic fields," Science **312**, 1780–1782 (2006).
9. A. V. Kimel, A. Kirilyuk, F. Hansteen, R. V. Pisarev, and T. Rasing, "Non-thermal optical control of magnetism and ultrafast laser-induced spin dynamics in solids," J. Phys.: Condens. Matter **19**, 043201 (2007).
10. S. A. Wolf, D. D. Awschalom, R. A. Buhrman, J. M. Daughton, S. von Molnar, M. L. Roukes, A. Y. Chtchelkanova, and D. M. Treger, "Spintronics: a spin-based electronics vision for the future," Science **294**, 1488–1495 (2001).
11. U. A. Khawaja and H. Stoof, "Skyrmions in a ferromagnetic Bose-Einstein condensate," Nature **411**, 918–920 (2001).
12. J. Baudon, M. Hamamda, J. Grucker, M. Boustimi, F. Perales, G. Dutier, and M. Ducloy, "Negative index media for matter-wave optics," Phys. Rev. Lett. **102**, 140403 (2009).
13. See, for example, spin-based techniques in M. A. Nielsen and I. L. Chuang, *Quantum Computation and Quantum Information* (Cambridge Univ. Press, 2000).
14. J. P. van der Ziel, P. S. Pershan, and L. D. Malmstrom, "Optically-induced magnetization resulting from the inverse Faraday effect," Phys. Rev. Lett. **15**, 190–193 (1965).
15. W. M. Fisher and S. C. Rand, Parametric Optical Magnetism and the Complex Mathieu Equation, in *Conference on Lasers and Electro-Optics/International Quantum Electronics Conference (IQEC'09)* OSA Technical Digest (CD) (Optical Society of America, 2009), paper ITuF3, http://www.opticsinfobase.org/abstract.cfm?URI=IQEC-2009-ITuF3.
16. W. M. Fisher and S. C. Rand, "Light-induced dynamics in an oscillator model with Lorentz forces," Phys. Rev. A (submitted).
17. B. Y. Zel'dovich, "Impedance and parametric excitation of oscillators," Phys. Usp. **51**, 465–484 (2008).
18. See, for example, I. I. Sobelman, *Atomic Spectra and Radiative Transitions* (Springer-Verlag, 1979).
19. Other applications of optical magnetism do not require operation near electronic resonances. The experiments of [1–3] indicate that by programming the intensity of irradiation, large spatial variations of magnetic susceptibility could be induced over wide spectral ranges of transparency, limited only by the bandwidth of available light sources. Hence transformation optics applications with low losses may be feasible at optical frequencies in unstructured, transparent materials. For spintronics, mid-gap irradiation of semiconductor hosts is capable of generating large internal magnetic fields to lock the spin orientation of conduction electrons and lengthen their decoherence times. Although the induced magnetic field reverses with each optical half-cycle, spin precession proceeds without spin flips if the optical magnetic field greatly exceeds the dephasing fields and is prealigned with the quantization axis. In this way, spin coherence can be extended over long (illuminated) paths.
20. See the review by M. Kauranen and S. Cattaneo, "Polarization techniques for surface nonlinear optics," in *Progress in Optics*, *Vol.* 51, E. Wolf, ed. (Elsevier, 2008), Chapter 2. No radiation is generated at the fundamental frequency or its second harmonic via a quadratic E^2 or B^2 nonlinearity in effectively centro-symmetric media like liquids. Only susceptibility elements for nonlinearities driven by an EB field combination are allowed. The susceptibility tensor for second-harmonic generation (SHG) in a bulk centro-symmetric medium does have a nonzero element χ_{zyx} for the field combination $B_y E_x$, which emits radiation perpendicular to the pump beam. However, the radiation is at 2ω, unlike the MD radiation reported at the fundamental frequency ω in liquid samples in [1,2]. In the present theory, the quantum mechanical symmetry requirement in a 2-level system is not inversion, but rather that $R(y)$ and x transform identically. The ED and MD transition moments must simultaneously be nonzero between states 1 and 2, which dictates that the initial and final states have opposite parity. In multilevel systems this rule may be relaxed by virtual transitions to other states, rendering the process partly allowed in the presence of complete inversion symmetry.
21. G. A. Mourou, C. P. J. Barty, and M. D. Perry, "Ultrahigh-intensity lasers: physics of the extreme on a tabletop," Physics Today **51**(1), 22–28 (1998).
22. Y. Kato, R. C. Myers, A. C. Gossard, and D. D. Awschalom, "Coherent spin manipulation without magnetic fields in strained semiconductors," Nature **427**, 50–53 (2003).
23. C. D. Stanciu, F. Hansteen, A. V. Kimel, A. Kirilyuk, A. Tsukamoto, A. Itoh, and Th. Rasing, "All-optical magnetic recording with circularly polarized light," Phys. Rev. Lett. **99**, 047601 (2007).
24. V. A. Stoica, Y.-M. Sheu, D. A. Reis, and R. Clarke, "Wideband detection of transient solid-state dynamics using ultrafast fiber lasers and asynchronous optical sampling," Opt. Express **16**, 2322–2335 (2008).